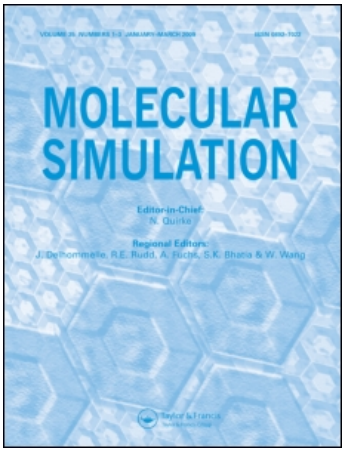

Molecular Simulation
Publication details, including instructions for authors and subscription information:
http://www.informaworld.com/smpp/title~content=t713644482

Deposition and Surface Dynamic of Metals Studied by the Embedded-Atom Molecular Dynamics Method

M. Katagiri[a]; A. Miyamoto[a]; T. R. Coley[b]; Y. S. Li[b]; J. M. Newsam[b]
[a] Tohoku University, Sendai, Miyagi, Japan [b] BIOSYM Technologies, INC., San Diego, California, USA

To cite this Article Katagiri, M. , Miyamoto, A. , Coley, T. R. , Li, Y. S. and Newsam, J. M.(1996) 'Deposition and Surface Dynamic of Metals Studied by the Embedded-Atom Molecular Dynamics Method', Molecular Simulation, 17: 1, 1 — 19
To link to this Article: DOI: 10.1080/08927029608024090
URL: http://dx.doi.org/10.1080/08927029608024090

Molecular Simulation, 1996, Vol. 17, pp. 1–19
Reprints available directly from the publisher
Photocopying permitted by license only

DEPOSITION AND SURFACE DYNAMIC OF METALS STUDIED BY THE EMBEDDED-ATOM MOLECULAR DYNAMICS METHOD

M. KATAGIRI and A. MIYAMOTO

Tohoku University, Sendai, Miyagi, Japan 980-77

T. R. COLEY, Y. S. LI and J. M. NEWSAM

BIOSYM Technologies, INC., San Diego, California 92121-3752, USA

(Received May 1995, accepted June 1995)

The embedded atom method (EAM) was used to simulate the dynamics of deposition of supported metal clusters on fcc transition metals and the dynamic behavior of surfaces. The formation of metal clusters was observed before deposition and the geometries, stabilities and dynamics of a series of metal clusters were discussed as obtained by EAM and compared with first-principle calculations. The calculations indicate that the structure of a cluster in the vapor phase is governed by its zero kelvin stability. We find that if the cluster forms in the vapor phase, it is difficult to get epitaxial growth since the metal cohesive energy is large and the cluster can not be broken by thermal motions. The effect of impurities on the deposition is also discussed. The anharmonicity, roughening and reconstruction of surface were also investigated. Three-body interactions were found to be important to understand these phenomena.

KEY WORDS: EAM, molecular dynamics, deposition, anharmonicity, roughening, reconstruction.

1 INTRODUCTION

Recently molecular dynamics (MD) algorithms which correspond to various ensembles have been proposed enabling a choice of thermodynamical control values. Realistic potentials like Allinger's MM3 [1] and Biosym's CFF93 force field [2, 3] being Class II force fields allow MD simulations of materials with covalent bonds. On the other hand, the Car-Parrinello method [4] which is a first principle MD technique has been developed and its future prospects are very promising. In addition, new techniques based on the density functional theory (DFT) like Effective-medium theory (EMT) proposed by Stott and Zaremba [5] and Norskov and Lang [6], Embedded-atom method (EAM) proposed by M. S. Daw and M. I. Baskes [7, 8] and developed by S. M. Foiles [9, 10] and Equivalent-crystal theory (ECT) introduced by Smith and Ferrante [11] have appeared. These methods may be applied to the design of real inorganic materials. Many interesting problems concerning metal clusters [12], grain-boundary segregation [9], liquid structure [10], surfaces [13], and others [14] have been investigated using the existing methods. In this work, we discuss application of EAM to the problem of deposition and related surface physics.

Since the artificial superlattice which is stacked up to form thin films has low dimension and periodicity, it is expected to exhibit unique physical properties (i.e. different from bulk crystals [15]). The dynamics of deposition or epitaxial growth on metal surfaces is related directly to phenomena such as surface diffusion, surface relaxation, surface anharmonicity and roughening, surface reconstruction, stability of metal clusters and sintering processes. To investigate these problems, it is necessary to use the "environment dependent" many-body interactions beyond the pair potential approximation. In this study, we investigated by MD using EAM potentials the dynamics of cluster formation, adsorption, diffusion and the effect of impurities during deposition.

2 METHODOLOGY

2.1 Embedded-atom Method (EAM)

M. S. Daw and M. I. Baskes developed a new technique, the embedded-atom method (EAM) on the basis of density functional theory, for calculating the structures and energetics of metals [7,8]. In this approach, the energy of the metal consists of the embedding energy and repulsive pair electrostatic interactions. The embedding energy is formulated as the energy required to immerse an atom in the local electron density provided by the remaining atoms.

$$E_{\text{coh}} = \sum_i F_i[\rho_{h,i}] + \frac{1}{2} \sum_{i,j(\neq i)} \phi_{ij}(R_{ij}) \tag{1}$$

In this expression, F is the embedding energy, $\rho_{h,i}$ is electron density due to the remaining atoms and ϕ is an electrostatic, pair interaction. $\rho_{h,i}$ is determined by superposition of electron density tails from the other atoms at its nucleus.

$$\rho_{h,i} = \sum_{j(\neq i)} \rho_j^a(R_{ij}) \tag{2}$$

The embedding energy includes many-body interactions which are represented as a function of derivatives of embedding energy derived from Taylor expansion of embedding energy about the average host electron density $\bar{\rho}$ [10].

$$\sum_i F(\rho_{h,i}) = NF(\bar{\rho}) + \sum_{\substack{i,j \\ (j\neq i)}} F_i'(\bar{\rho})[\rho_j^a(R_{ij}) - \delta] + \frac{1}{2} \sum_{\substack{i,j \\ (j\neq i)}} F_i''(\bar{\rho})[\rho_j^a(R_{ij}) - \delta]^2$$

$$+ \frac{1}{2} \sum_{\substack{i,j,k \\ (k\neq j\neq i\neq k)}} F_i''(\bar{\rho})[\rho_k^a(R_{ik}) - \delta][\rho_j^a(R_{ij}) - \delta] \tag{3}$$

where

$$\rho_{h,i} = \bar{\rho} + \sum_{j(\neq i)} [\rho_j^a(R_{ij}) - \delta] \tag{4}$$

$\delta = \bar{\rho}/(N-1)$ and N is the number of atoms in the system. The summation in the last term of (3) avoids coincidence of any two of the summation indices. Also, F' and F'' represent the first two derivatives of the embedding energy of atom i, with respect to the electron density evaluated at $\bar{\rho}$. The final term represents the three-body contributions and three-body interaction is proportional to F''.

Since the slope of the embedding function is negatively infinite at $\rho_{h,i} = 0$ and has positive value large at high density region [16], F'' is positive and the three-body interactions are always positive and exponentially decaying. As a result, three body interactions are repulsive while pair interactions are attractive. This is a general feature of EAM and the existence of many-body interactions makes the potential different in the surface and cluster region from that in the bulk region. Figure 1 shows the cohesive energies and embedding functions of fcc metals. The cohesive energy of fcc metals were estimated by Rose *et al.* [17] and the EAM parameters were fitted by Foiles, Baskes and Daw [18]. In Figure 1, the curvature of embedding function for Pt and Au is relatively large. Since the three-body interaction is proportional to this curvature, the behavior of Pt and Au in quite different from the one derived from the pair potential approximation [14]. Thus we can treat "environment-dependent" structure and the bonds of surface atoms or cluster atoms with lower coordination numbers appear to be stronger and shorter than that of bulk atoms.

2.2 *Interprocess Communication (IPC)*

EAM has been used as a tool for calculating interactions. This interaction part has been incorporated as a function part of Discover (BIOSYM Technologies, INC.) and

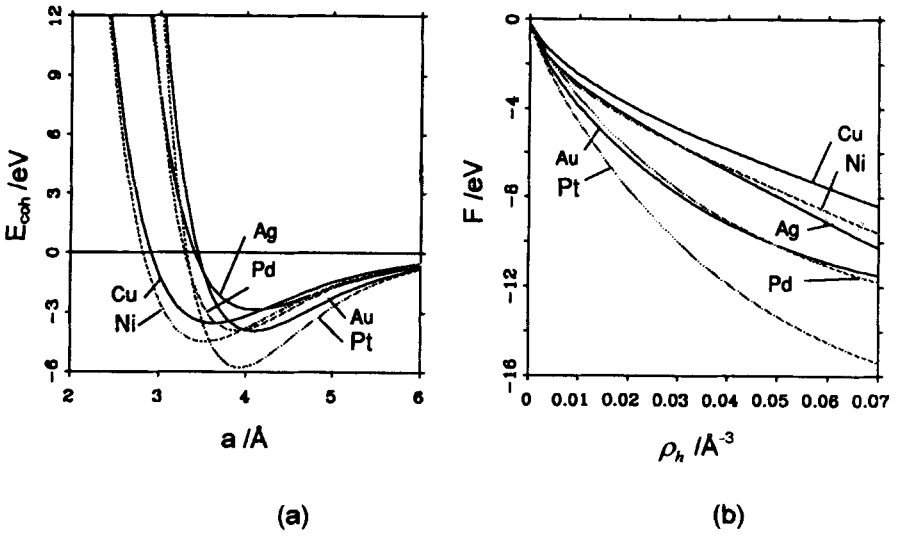

Figure 1 Cohesive energies and embedding function of fcc metals [8]. (a) Cohesive energy (in eV) as a function of lattice constant (in Å). (b) Embedding energy (in eV) as a function of electron density (in Å^{-3}). The three-body interaction is proportional to the second derivative of the embedding function and is always positive in EAM. The behavior of Pt and Au is different from the one derived from pair potential [10, 14].

communicates with Discover through bi-directional, named pipe-based interprocess communication (IPC). Such arrangement provides an interesting example of employing an external energy evaluation as an aid to a generalized open simulation system and interprocess communication protocols. As the development of basic formalisms for both, classical and quantum mechanical interactions, any techniques which estimate energies and derivatives at each atom can be used. Our study is an example where the EAM is used as the generator of interactions. The objectives of this work are: (a) Properties of isolated clusters like geometries, stabilities, dynamics and chemistry; (b) Physical and chemical influence of supports; (c) Flexible approaches to simulations of such complex systems such as semi-classical, quantum and combined classical-semi-classical-quantum; (d) Imposed insights and simulation protocols for supported metal chemistry and physics.

3 DYNAMICS BEFORE DEPOSITION

Schneider, Rahman and Schuller [19] studied the vapor deposition of LJ atoms, and Gilmore and Sprague [20] studied this using EAM. These successive studies focused on the deposition with energetic atoms and revealed the dynamics of layer growth. In this paper we elucidate the relation between cluster growth in the vapor phase and layer growth on the substrate. To consider this relation without energetic effects, we selected the randomly disordered vapor phase as the initial structure. We applied EAM MD to the deposition of Cu on Pt(110) surface. The basic cell parameters were $a = 31.3920$ Å, $b = 33.2960$ Å and $c = 50.0$ Å. The C-axis was vertical to the surface. The numbers of Cu and Pt were 189 and 384, respectively, and the number of Pt layers was 4. This layer size is in principle not sufficient to simulate the dynamics on the surface since the energetic influence of up to 10 layers was estimated to be significant. However, the main purpose of this section is to simulate the dynamics before deposition and bigger surface model was used to study the dynamics on the surface. To get the initial structure, we prepared the random vapor phase of Cu at very high temperature with all Pt atoms fixed. Then we simulated the deposition process at the destination temperature while relaxing Pt atoms except the fixed bottom layer. Cu atoms had no incident energies towards the surface. Figure 2 shows a snapshot at 700 K. Both atoms and clusters adsorbed onto the Pt surface could be observed. It can be seen from Figure 2 that the existence of the Cu_{19} cluster has the highest probability at this initial density of Cu and that this cluster was formed at early times. This cluster remained in the vapor phase for a long time while atoms not involved into the cluster were deposited on the surface earlier due to the mass effect. The destruction of clusters in the vapor phase was not observed at this temperature. Figure 3(a) shows the cohesive energy of Cu clusters in vacuum as a function of the number of atoms at zero temperature. These structures were obtained by simulated annealing (SA) technique. Figure 3(b) shows the second derivative of the cohesive energy. For comparison the results of first principle calculation using DMol are displayed. During DMol calculations, no symmetry was imposed to account for Jahn-Teller distortion. It follows from Figure 2 and Figure 3, that the structure of clusters formed before deposition is governed by the zero kelvin stability of the cluster even at finite temperatures. It has been shown that the electronic temperature may have

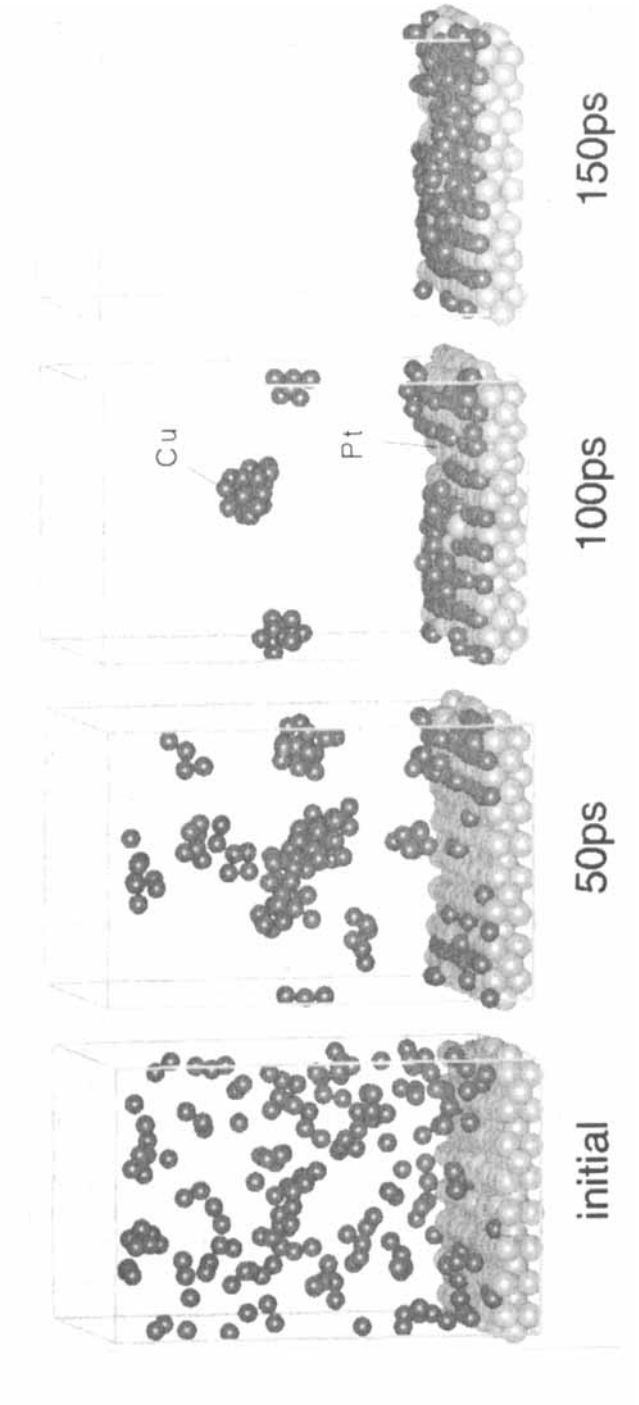

Figure 2 Deposition of Cu on Pt(110) at 700 K. The existence of Cu_{19} cluster has the highest probability and this corresponds with the stability of cluster shown in Figure 3. See color plate I.

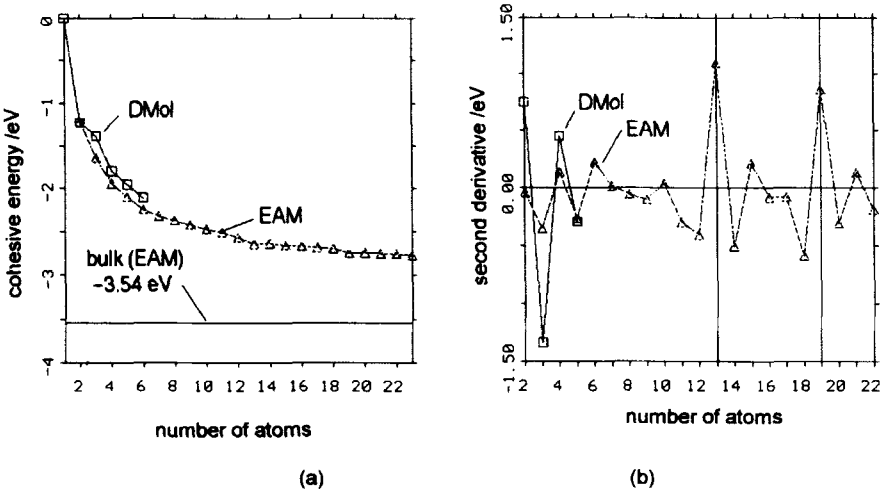

Figure 3 Cohesive energy and it's second derivative of Cu cluster. (a) Cohesive energy (in eV) as a function of the number of Cu atoms in cluster. (b) Second derivative of (a) (in eV). The results calculated by DMol as a first-principle calculation are also shown. Cu_{13} and Cu_{19} are relatively stable in this EAM.

important effects if there are large level degeneracies of some clusters [21]. This means that entropy effects smear out magic numbers at high temperatures. However, large level degeneracies have not been seen for the Cu cluster [22]. This indicates that the EAM is an adequate representation for Cu clusters at finite temperature.

Nevertheless, there remain some doubts while reconstructing very small clusters using EAM. In Figure 4 we show several geometry optimized structures of Cu clusters and cluster cations by using first-principle code DMol. All structures were optimized without using any spin and symmetry constraints. The DNP atomic basis set was used and gradient corrections to exchange-correlation were not considered. For cations, we show the most stable structures only. For Cu_3, the isosceles triangle is more stable than the regular triangle, while for Cu_3^+, the regular triangle is more stable than the isosceles triangle. It is difficult to converge the energy without adding perturbation between orbitals which are close to the Fermi level, since HOMO and LUMO of Cu_3 are very close (HOMO = -3.906 eV, LUMO = -3.900 eV) and the energy oscillates during energy optimization. On the contrary, for Cu_3^+ where HOMO (-11.183 eV) and LUMO (-8.861 eV) are not close, the distortion doesn't occur. In this calculation, we did not use any symmetries and the energy levels did not degenerate fully for the regular triangle Cu_3. If we use the D_{3H} symmetry, the energy levels degenerate exactly. Then the electron occupation for degenerate orbitals is fractional and the charge distribution becomes non-spherical. This causes distortion of the structure to get lower symmetry (Jahn-Teller effect). This Jahn-Teller distortion occurs even for larger clusters. Moreover, the structure of Cu_n clusters (n is less than 7) is basically planar as obtained from DMol, since Cu has one 4s electron in the outer shell. The results are the same as for Na clusters. This result of planar structure indicates the existence of bond directions in very small Cu clusters. Within EAM, it is difficult to reconstruct these planar and distorted

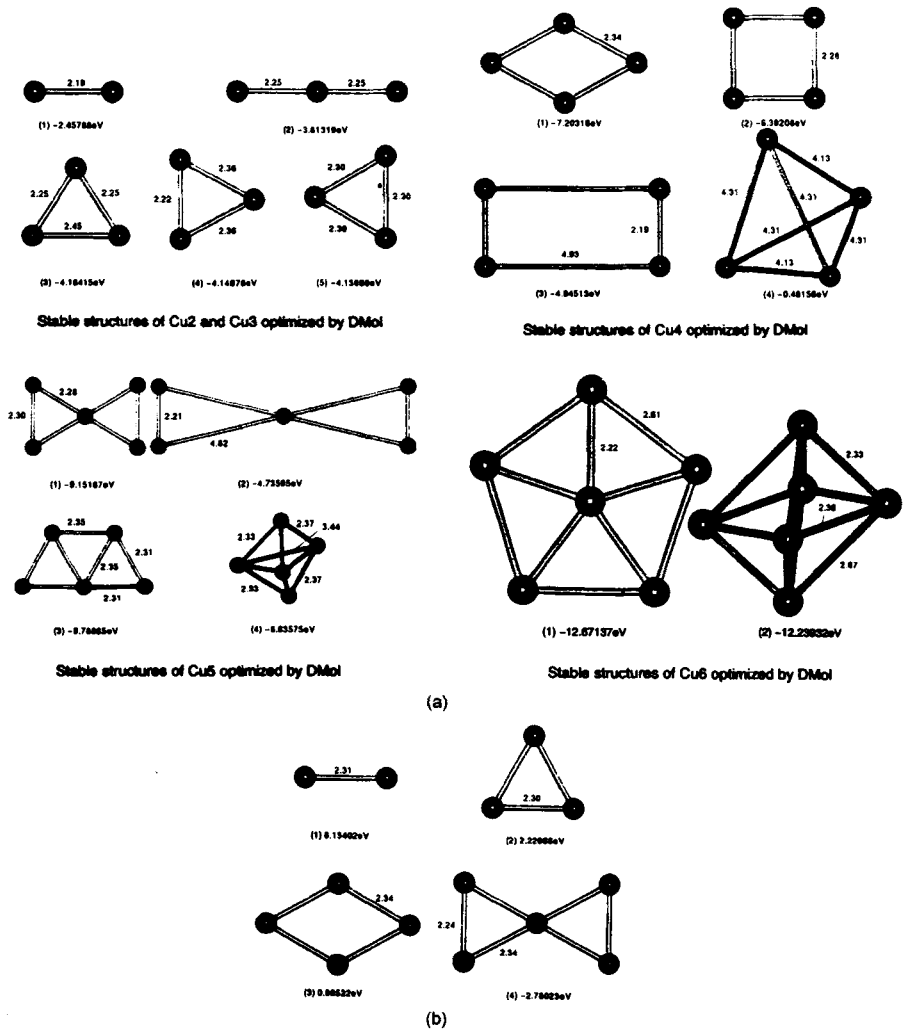

Figure 4 Stable structures of Cu cluster calculated by DMol. (a) Cu cluster (b) Cu cation cluster. The bond lengths are in unit of Å. Binding energies are also shown. The most stable structures are basically planar up to Cue. For Cu_3, the isosceles triangle is more stable than the regular triangle because of Jahn-Teller distortion while Cu_3^+ is regular triangle. See color plate II.

structures but the estimation of cohesive energy is very good. Moreover, the bond length given by EAM is shorter for smaller clusters, since EAM uses the "environment-dependent" potential as mentioned above. Figure 5 shows the optimized structures of Cu clusters using EAM. Within EAM, Cu_{13} and Cu_{19} are relatively stable (magic numbers = 13, 19). The most stable structures of Cu_{13} and Cu_{19} are the icosahedron and double icosahedron, respectively. The structures of Cu_{12} and Cu_{14} are obtained from Cu_{13} icosahedron by removing a surface atom and adding an atom over a triangular face, respectively. However, within the effective medium approach with

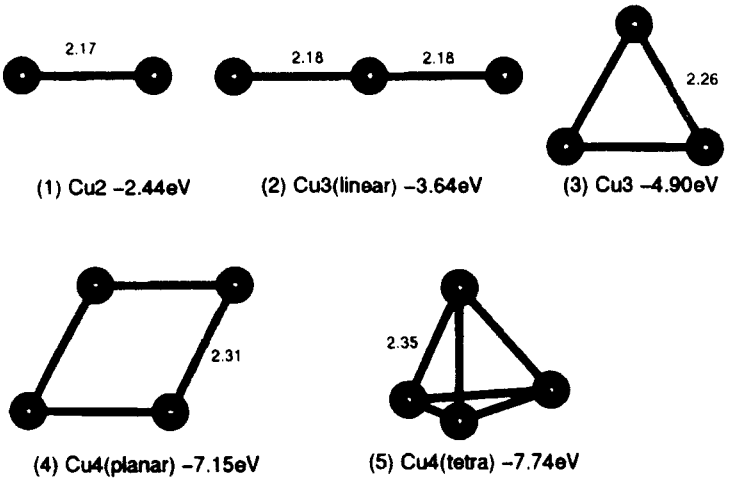

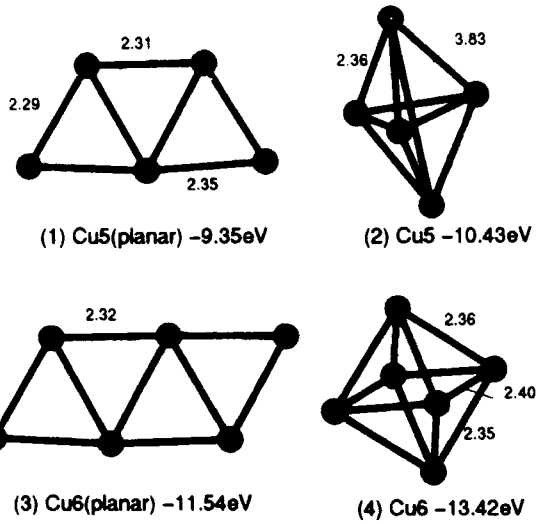

Figure 5 Stable structures of Cu cluster by EAM. To predict the correct magic number of Cu cluster, it is necessary to consider the electronic shell structure [22].

corrections for electronic shell structure, Cu_8, Cu_{18} and Cu_{20} are relatively stable (magic number 8, 18, 20) and only Cu_8 and Cu_{20} and the close-packed Cu_{13} are almost spherical [22]. Experiment also supports this result [23]. While magic numbers for the very small cluster are inaccessible by EAM, it is able to reproduce the most stable

structure of Cu_{13}. From DMol, the geometrically optimized configurations have binding energies of 34.1 eV for the icosahedral structure, 34.0 eV for the fcc structure and 33.4 eV for the hcp structure [24]. Using EAM, only the icosahedral structure was obtained by SA and has the binding energy of 34.1 eV as shown in Figure 6.

Contrary to this difference of magic numbers for Cu clusters, the stability of Pd clusters which have strong cohesive energy and a many-body long-ranged force can be predicted by the many-body alloy (MBA) potential [25] which is similar to EAM. The most stable structure of a Pd cluster is a close-packed one. For example, Pd_4 is a tetrahedron while Cu_4 is planar. Metallic bonds tend to delocalize the electron distribution. However, the degree of electron delocalization of clusters is very different between Pd which has unoccupied *d* orbitals and Cu which have no unoccupied *d* orbitals. The difference between the metallic bond and the covalent bond is not clear since we can not define the band gap exactly in small clusters. However we can say that very small Cu clusters exhibit bond direction. We recognise this deficiency of EAM and improve the EAM further so that it applies to bond-direction systems such as very small Cu clusters. However, for the large Cu clusters (smaller than 2000), the effective-medium theory without corrections for shell structure by Valkealahti and Manninen [26] gives the icosahedron as energetically the most stable structure and the result is in good agreement with the electronic diffraction results of Reinhard *et al.* For very small clusters, we can apply the first-principle calculations directly. Moreover, the attempt to combine quantum mechanical technique with classical technique has started [27].

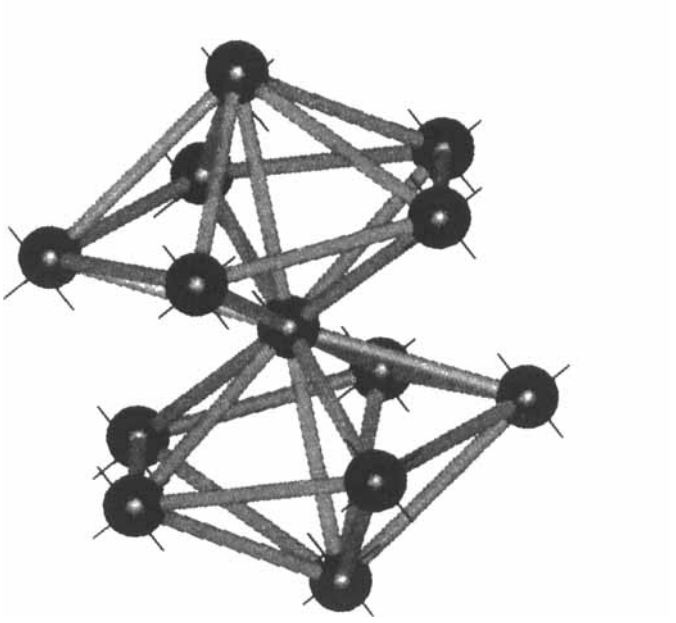

Figure 6 Icosahedral structure of Cu_{13} by DMol(CPK) and EAM(CROSS). The close-pack icosahedral Cu_{13} structure is well reproduced by EAM. The binding energy by DMol is 34.1 eV (See Ref. 24) and 34.1 eV by EAM. See color plate III.

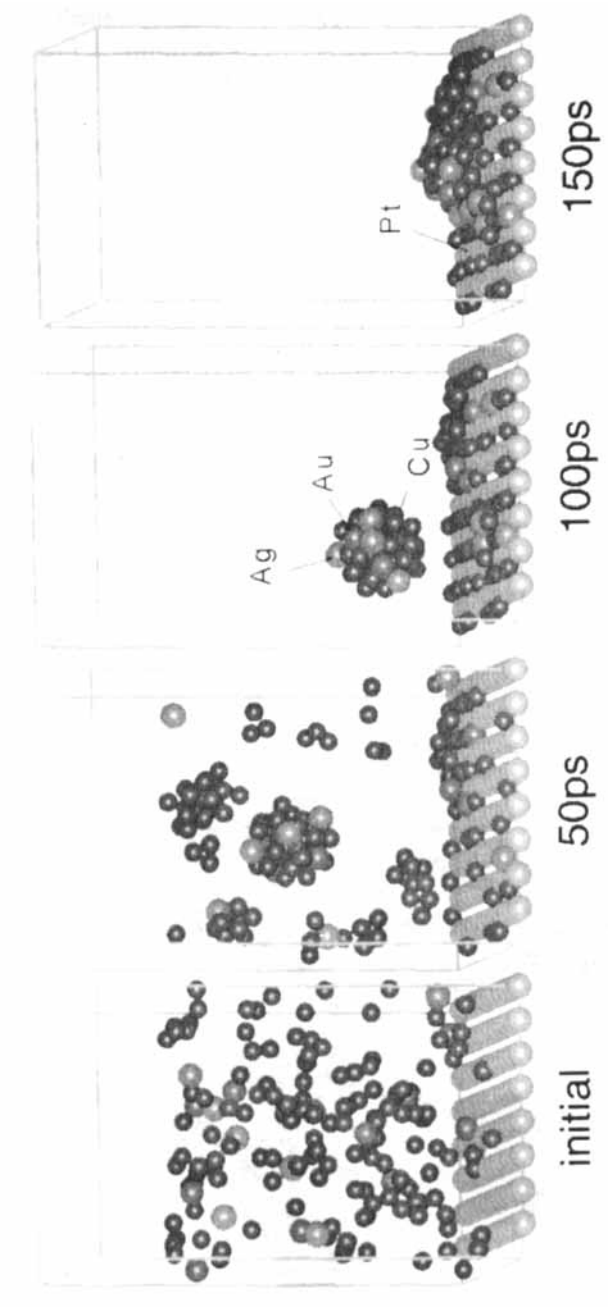

Figure 7 Deposition of Cu on Pt(110) surface at 700 K in the existence Ag and Au. This is the case of adding Ag and Au atoms as impurities to Figure 2. The bigger cluster was formed compared to Figure 2. See color plate IV.

We simulated the effect of impurities on the structure of clusters and on the deposition. The structures of cluster and the finally obtained adsorbates are strongly influenced by the existence of impurities. Figure 7 illustrates the case when Ag (14 atoms) and Au (14 atoms) are added as impurities to pure Cu vapor phase. In this case, the observation of adsorbates of atoms and clusters is the same as in Figure 2. However, a bigger cluster (Cu = 47, Ag = 4, Au = 5) was observed than in the pure Cu growth case. The existence of impurities makes it difficult to get epitaxial growth, as the cluster tends to become bigger with impurities than in a pure copper only system. Hence cluster fragmentation does not occur because of strong metallic cohesive energy. Figure 8 shows a snapshot of the cluster. The impurities tend to exist in the outer shell of the cluster. For this small cluster, no obvious surface exists. However, if the cluster is much bigger, then the surface structure appears [28]. The atoms which have weaker cohesive energy like Ag tend to exist in the outer shell, especially at the edge [29].

4 DYNAMICS OF ADSORBATES

Figure 9 shows the snapshots of adsorbed Pt and Ag atoms on Cu(110) surface at 900 K. Two Pt clusters having 63 atoms each were put on the Cu(110) surface and the sintering process for 200 ps (1 step = 3 fs) was observed. The same was repeated for two 63-atom Ag clusters on Cu(110) surface.

In the case Pt cluster, the sintering process was observed and the sintered structure was retained. This process seems to be separated into two processes. One is surface

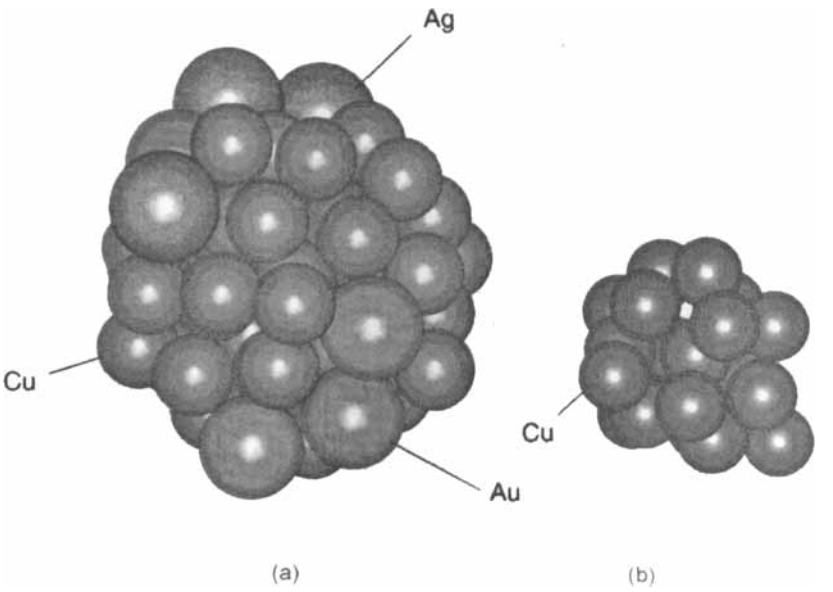

Figure 8 Formed cluster in vapor phase during the deposition in Figure 2 or Figure 7. (a) in the presence of impurities (Fig. 7) $Cu_{47}Ag_4Au_5$ cluster was formed. (b) pure Cu system (Fig. 2). Cu_{19} cluster was formed. See Color Plate Va.

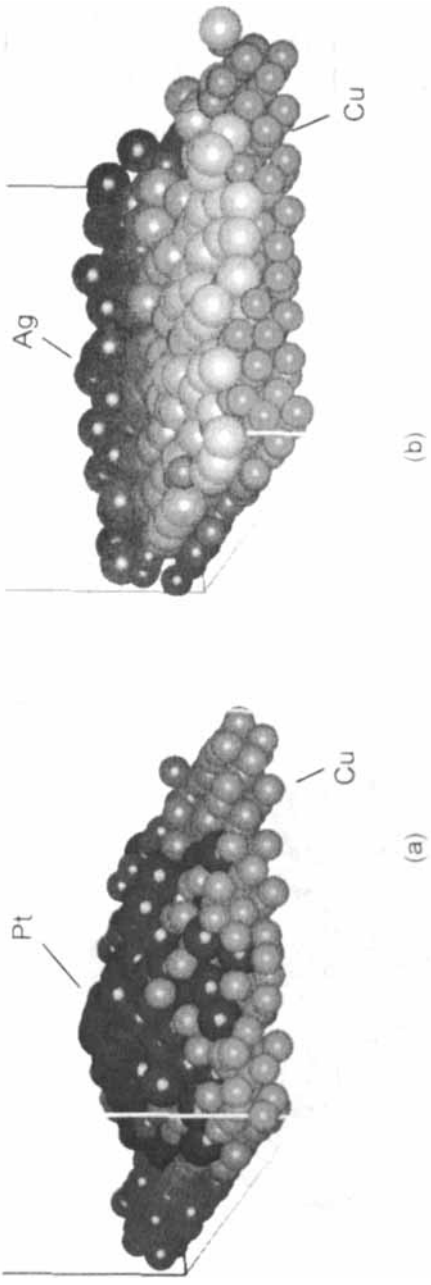

Figure 9 Snapshot of Pt and Ag clusters on Cu(110) at 900 K. (a) Pt_{63} cluster on Cu(110) (b) Ag_{63} cluster on Cu(110) Simulations were carried out for 200 psec. By the differences of cohesive force, Cu atoms diffused on the "surface" of Pt_{63} cluster in (a) while the mutual diffusion was observed between Ag and Cu because of the weak cohesive force of Ag. 900 K is in the anharmonic vibration region of Cu(110). See color plate V.

diffusion and the other one is sintering. We observed that the diffusion of Pt cluster is very slow while the atoms in the cluster move actively, and if two clusters get within the cut-off length, rapid sintering occurs. Therefore the sintering time depends on the initial coordinates of the two clusters. The difference between simulated and experimental sintering times may be explained by this. Moreover, Cu atoms constituting the surface, separate from surface, and diffuse on the sintered Pt cluster to get a potentially stable structure with Pt.

In the case of Ag clusters, mutual diffusion between Ag and Cu atoms was observed without Ag cluster sintering, since the cohesive energy of Ag is weak and the interaction between Ag and Cu is stronger than that among Ag. We can say that the structure and dynamics of metal clusters on the surface is strongly influenced by the potential relation between the adsorbate and the surface.

This behavior is influenced by the anharmonicity of surface atoms. On the Cu(110) surface, the motion of atoms change significantly in the region around 550 K. Such experimental factors as He scattering [30, 31], photo emission [32], low-energy ion scattering [33], inverse photo emission [33], and X-ray scattering intensities [34] decrease significantly faster than it is predicted by a simple Debye-Waller factor at temperatures higher than 550 K. This effect was explained by a contribution of anharmonicity of the vibrations at the surface [31]. Recently the three regions of temperature effects ($T_1 = 700$ K and $T_2 = 1000$ K) were reported using directional elastic peak electron spectroscopy (DEPES) and directional auger electron spectroscopy (DAES) for Cu(110) surface [35]. The lower temperature was ascribed to the appearance of anharmonic thermal vibrations while the second one indicated the surface roughening transition. These studies indicate the existence of anharmonic regions and roughening regions before melting. We investigated the layer relaxation of the Cu surface to make clear the surface anharmonic and roughening effects on the deposited cluster. We show the layer relaxation of Cu surfaces and relative layer spacing d_{12}/d in Figure 10 (d_{12} is layer spacing between first and second layer and d is the bulk interplanar spacing). Ten layer systems were used and the bottom layer was fixed during relaxation. In the case of the layer spacing d_{12} for Ag(111), the experiment using medium-energy ion scattering (MEIS) results [36] gave d_{12} crossing the other ones at low temperature. This behavior was not reproduced by EAM calculation [37] while effective medium calculation succeeded in reproducing the Cu(110) surface [38]. EAM, gives the layer spacing d_{12} too small and the surface contracts too much. Nevertheless, the anharmonic effect seems to occur around 700 K and the roughening effect seems to occur around 1000 K for Cu(110) surface before melting (melting temperature is 1358 K). The influence of surface anharmonic effect on the surface energy should not be greater than that of surface roughening effect shown in Figure 11. Figure 11 shows surface energies as a function of temperature. The experimental value of surface energy for the averaged face is 1790 erg/cm^2. The anharmonic effect is not as clearly visible as the roughening effect on the basis of surface energy. However, this anharmonicity influences strongly the structure of adsorbates on the surface. Figure 12 shows the snapshots of sintered Pt_{126} clusters on Cu(110) surface at 500 K and 900 K. Simulations were carried out for 200 ps (1 step = 3 fs) respectively. The diffusive motion of Cu on Pt cluster "surface" was observed at 900 K while Cu atoms couldn't overcome the potential barrier and stayed at the initial positions within this time period at 500 K.

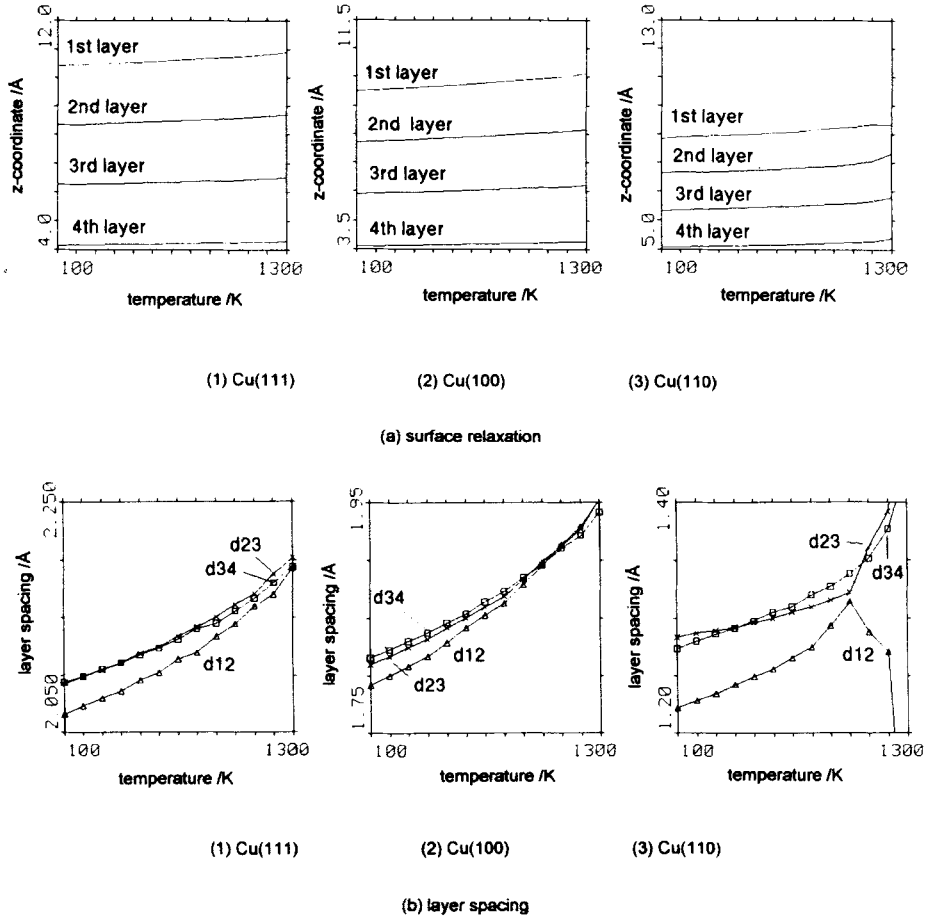

Figure 10 Layer relaxations and layer spacings of Cu surfaces. (a) Surface relaxation (in Å) as a function of temperature (in K). (b) Layer spacings (in Å) as a function of temperature (in K).

The structure of Pt cluster tended to be planar at 900 K compared to 500 K. At lower temperatures, the structure of a supported cluster is not spherical and the surface structure reflects in the cluster, ordered to correspond with substrate structure. Considering the high melting point of Pt ($T_m = 2042$ K), this difference was considered to be caused mainly by the influence of the Cu atoms.

In considering the structure of deposition growth, surface roughening is important since this phenomenon increases the activation energies of mobility of adatoms [39]. Moreover, in treating the surface system in which the three-body interaction is important, we face another problem, namely clean surface reconstruction. For example, Au(110) or Pt(110) surfaces reconstruct to (1X2) superstructures, while the Cu(110) surface does not reconstruct in the absence of adsorbates. Before investigating the influence of reconstruction on the dynamics of adsorbates, we carried out the

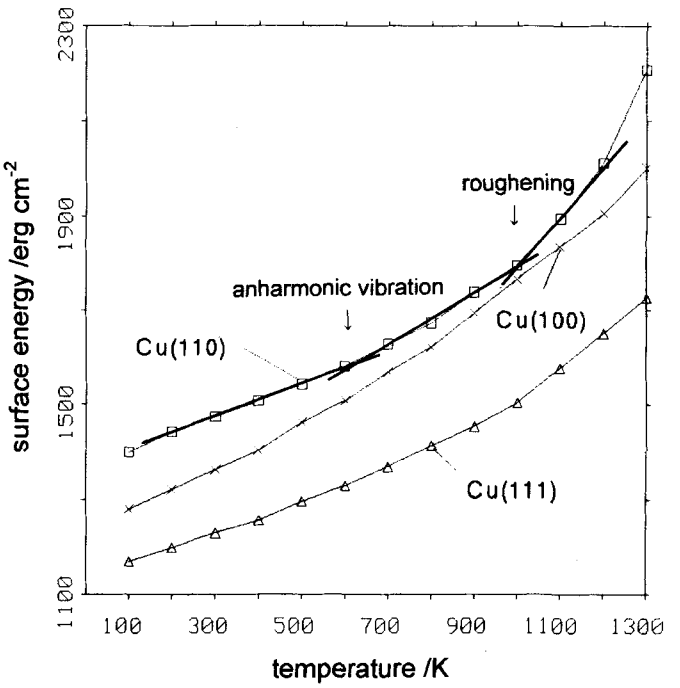

Figure 11 Surface energies (in erg/cm^2) of Cu as a function of temperature (in K). For Cu(110), the anharmonic vibration region and roughening region start from about 600 K and 1000 K respectively.

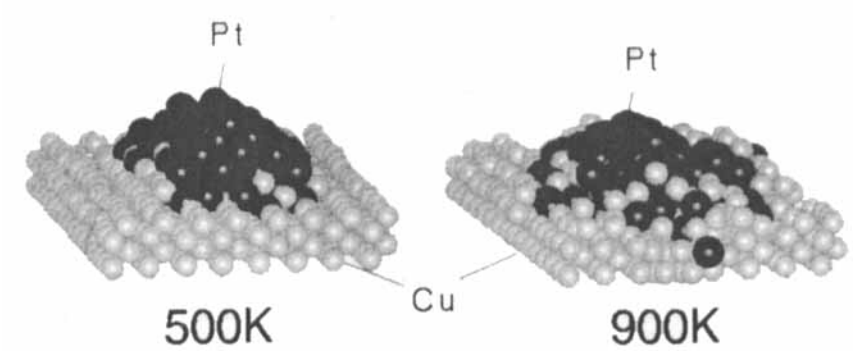

Figure 12 Snapshot of Pt_{126} cluster on Cu(110) at 500 K and 900 K. Cu atoms diffuse on the surface of Pt_{126} cluster in the anharmonic region (900 K) while this diffusion was not observed in the simulation time (200 psec) at 500 K. See color plate VI.

simulation on Pt(110) surface system without adsorbates at 1800 K as shown in Figure 13. Experimentally, the missing-row critical temperature for Pt(110) has been measured at 960 K [40]. Simulations were carried out for 90 ps (1 step = 3 fs). Experimentally, the $(1 \times 2) \Leftrightarrow (1 \times 1)$ rearrangement is reversible, thus the energy change

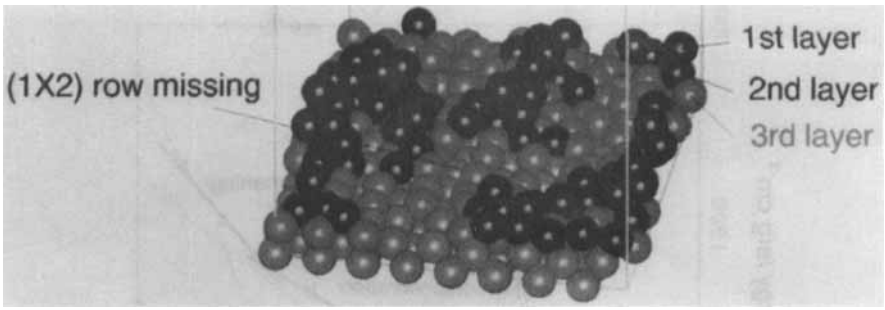

Figure 13 Structure of Pt(110) surface reconstruction at 960 K. Simulation was carried out for 90 psec. See color plate VII.

accompanying the rearrangement seems to be small. This energy difference is only $-2\,\text{meV/Å}^2$ for Pt(110) where the rearrangement from (1×1) to (1×2) is profitable energetically while the energy change fo Cu(110) is $1\,\text{meV/Å}^2$ and the process is not profitable energetically [14]. When the reconstruction occurs, the number of second neighbor atoms decreases and the process is not profitable energetically from the viewpoint of effective pair potential (attractive), however, it is profitable energetically from the viewpoint of effective three body interaction (repulsive) [14]. The reconstruction phenomena occurs for the species which have strong cohesive energy and strong three-body interaction like Pt and Au. Therefore, three-body interaction is important to consider the reconstruction phenomena. This reconstruction influences the dynamics of adsorbed cluster or atoms. In Figure 13, the configuration seems to be amorphous-like structure. It is difficult to get the fine rearrangement structure by MD since the energy change due to the rearrangement is small and the process is reversible experimentally. The temperature we used was a little high to get fine structure. There is another reconstruction type that is adsorption induced reconstruction. This reconstruction is observed at very lower temperature below the anharmonic vibration region. Cu(110)-(2×1)O reconstruction induced by the adsorption of oxygen on Cu(110) was observed even at 200 K and the Cu atoms move as a linear unit away from the step. This was studied on the catalytic CO–O_2 and CO–NO reactions on Cu(110) by reactive oxygen species at low temperatures using MS, AES, LEED and HREELS [41]. They found that the catalytic CO oxidation proceeded on an unreconstructed Cu(110) between 200 and 230 K and the (2×1)-O phase which was not reactive was produced above 200 K. Its growth caused a decrease of the number of clean sites, leading to inhibition of the reaction. 200 K is less than the temperature which caused the anharmonic vibration of Cu(110) surface atoms and the diffusion should be very low. The mechanism of the adsorption induced reconstruction is different from the clean surface reconstruction which we simulated, since the former case is strongly related to the interaction between surface atoms and the adsorbed atoms. At 200 K, the diffusion of Cu atoms is very low and the initial mechanism of the reconstruction should be the interaction between Cu and adsorbed atoms. It is very important to treat this reconstruction phenomena when we consider the surface reactions and other related surface physics like AFM.

5 SUMMARY

The study of metal deposition includes several elementary processes like cluster growth, adsorption, diffusion, sintering, and surface reconstruction and the deposition is essentially a non-equilibrium processes. In this work, we tried to describe the deposition process including surface dynamics using the embedded-atom molecular dynamics method. We have found the cluster created in the vapor phase is governed by the 0 K stability of the cluster. The cluster formed in vapor phase is stable and it cannot be destroyed on the surface at the simulated temperatures because of strong metal cohesion. After deposition, the dynamics of the cluster is influenced by the anharmonic and roughening effects of the surface. In the anharmonic region, the diffusion of surface atoms on the deposited cluster was observed. Moreover, the dynamics of the cluster is influenced by the relative of strengths of the interaction between the surface and the cluster. If the interaction between the cluster and the surface is stronger than that within clusters, mutual diffusion of cluster atoms and surface atoms is observed. In contrast, when the interaction between the cluster and the surface is weaker than that among clusters, sintering is observed. Finally we can conclude that both the cohesive energy relation and many-body interactions are important in the deposition growth. It is necessary to estimate the "environment dependent" cohesive energy differently from bulk using many-body interactions to investigate the dynamics of deposition process, since the deposition process is essentially one characteristic of non-bulk systems.

Acknowledgments

It is a pleasure to thank Minoru Tanaka, Nick Quirke, Behnam Vessal, Sundar Veliah, Lalitha Subramanian, M. A. van Daelen and Ewa Broclawik for valuable discussions and David U. Martin and Jon N. Hurley for developing IPC procedure.

References

[1] N. L. Allinger, Y. H. Yuh and J.-H. Lii, "Molecular mechanics – The MM3 force field for hydrocarbons, 1", *J. Am. Chem. Soc.*, **111**, 8551 (1989).

[2] J. R. Maple, M.-J. Hwang, T. P. Stockfisch, U. Dinur, M. Waldman, C. S. Ewig and A. T. Hagler, "Derivation of class II force fields. 1. Methodology and quantum force field for the alkyl functional group and alkane molecules", *J. Comp. Chem.*, **15**, 162 (1994).

[3] M. J. Hwang, T. P. Stockfisch and A. T. Hagler, "Derivation of class II force field 2. Derivation and characterization of a class II force field, CFF93, for the alkyl functional group and alkane molecules", *J. Am. Chem. Soc.*, **116**, 2515 (1994).

[4] R. Car and M. Parrinello, "Unified approach for molecular dynamics and density-functional theory, *Phys. Rev. Lett.*, **55**, 2471 (1985).

[5] M. J. Stott and E. Zaremba, "Quasiatoms: An approach to atoms in nonuniform electronic systems", *Phys. Rev.*, **B22**, 1564 (1980).

[6] J. K. Norskov and N. D. Lang, "Effective-medium theory of chemical binding: Application to chemisorption", *Phys. Rev.*, **B21**, 2131 (1980).

[7] M. S. Daw and M. I. Baskes, "Semiempirical, quantum mechanical calculation of hydrogen embrittlement in metals", *Phys. Rev. Lett.*, **50**, 1285 (1983).

[8] M. S. Daw and M. I. Baskes, "Embedded-atom method: derivation and application to impurities, surfaces, and other defects in metals", *Phys. Rev.*, **B29**, 6443 (1984).

[9] S. M. Foiles, "Calculation of grain-boundary segregation in Ni-Cu alloys", *Phys. Rev.*, **B40**, 11502 (1989).
[10] S. M. Foiles, "Application of the embedded-atom method to liquid transition metals", *Phys. Rev.*, **B32**, 3409 (1985).
[11] J. R. Smith, T. Perry, A. Banerjea, J. Ferrante and G. Bozzolo, "Equivalent-crystal theory of metal and semiconductor surfaces and defects", *Phys. Rev.*, **B44**, 6444 (1991).
[12] A. Sachdev, R. I. Masel and J. B. Adams, "Embedded-atom calculations of the equilibrium shape of small platinum clusters", *J. Catalysis*, **136**, 320 (1992).
[13] C. L. Liu, J. M. Cohen, J. B. Adams and A. F. Voter, "EAM study of surface self-diffusion of single adatoms of fcc metals Ni, Cu, Al, Ag, Au, Pd and Pt", *Surface Science*, **253**, 334 (1991).
[14] M. S. Daw, S. M. Foiles and M. I. Baskes, "The embedded-atom method: a review of theory and applications", *Materials Science Reports*, **9**, 251 (1993).
[15] A. Maeda, T. Satake, T. Fujimori and H. Kuroda, "Epitaxial growth of bcc-Eu/Yb superlattices", *J. Appl. Phys.*, **68**, 3246 (1990).
[16] M. J. Puska, R. M. Nieminen and M. Manninen, "Atoms embedded in an electron gas: Immersion energies", *Phys. Rev.*, **B24**, 3037 (1981).
[17] J. H. Rose, J. R. Smith, F. Guinea and J. Ferrante, "Universal features of the equation of state of metals", *Phys. Rev.*, **B29**, 2963 (1984).
[18] S. M. Foiles, M. I. Baskes and M. S. Daw, "Embedded-atom-method functions for the fcc metals Cu, Ag, Au, Ni, Pd, Pt and their alloys", *Phys. Rev.*, **B33**, 7983 (1986).
[19] M. Schneider, A. Rahman and Ivan K. Schuller, "Role of relaxation in epitaxial growth: a molecular-dynamics study", *Phys. Rev. Lett.*, **55**, 604 (1985).
[20] C. M. Gilmore and J. A. Sprague, "Molecular-dynamics simulation of the energetic deposition of Ag thin films", *Phys. Rev.*, **B44**, 8950 (1991).
[21] M. Brack, O. Genzken and K. Hansen, "Thermal properties of the valence electrons in alkali metal clusters", *Zeitschrift Fur Physik*, **D21**, 65 (1991).
[22] O. B. Christensen, K. W. Jacobsen and J. K. Norskov, "Cu cluster shell structure at elevated temperatures", *Phys. Rev. Lett.*, **66**, 2219 (1991).
[23] J. Garcia-Rodeja, C. Rey, L. J. Gallego and J. A. Alonso, "Molecular-dynamics study of the structures, binding energies, and melting of clusters of fcc transition and noble metals using the Voter and Chen version of the embedded-atom model", *Phys. Rev.*, **B49**, 8495 (1994).
[24] Y. S. Li, M. A. van Daelen, M. Wrinn, D. King-Smith, J. M. Newsam, B. Delly, E. Wimmer, T. Klitsner, M. P. Sears, G. A. Carlson, J. S. Nelson, D. C. Allan and M. P. Teter, "Density functional methods as computational tool in materials design", *Journal of Computer-Aided Materials Design*, **1**, 199 (1993).
[25] Y. S. Li, Y. Cai and J. M. Newsam, "Structure and growth of small Palladium clusters", in Materials Theory and Modelling (*Mat. Res. Sco. Symp. Proc.* **291**), J. Broughton, P. Bristowe and J. M. Newsam, eds., Materials Research Society, Pittsburgh, 1983, pp. 573.
[26] S. Valkealahti and M. Manninen, "Instability of cuboctahedral copper clusters", *Phys. Rev.*, **B45**, 9459 (1992).
[27] C. M. Koelmel, Y. S. Li, C. M. Freeman, S. M. Levine, M.-J. Hwang, J. R. Maple and J. M. Newsam, "Quantum and molecular mechanics study of the tris (quaternary ammonium) cation used as the zeolite ASM-18 synthesis template", *J. Phys. Chem.*, **98**, 12911 (1994).
[28] S. Valkealahti and M. Manninen, "Simulation of cluster growth using a lattice gas model", *Phys. Rev.*, **B50**, 17564 (1994).
[29] M. Katagiri *et al.* (in preparation).
[30] D. Gorse and J. Lapujoulade, "A study of the high temperature stability of low index planes of copper by atomic beam diffraction", *Surf. Sci.*, **162**, 847 (1987).
[31] P. Zeppenfeld, K. Kern, R. David and G. Comsa, "No thermal roughening on Cu(110) up to 900 K", *Phys. Rev. Lett.*, **62**, 63 (1989).
[32] R. S. Williams, P. S. Wehner, J Stöhr and D. A. Shirley, "Thermally induced breakdown of the direct-transition model in copper", *Phys. Rev. Lett.*, **39**, 302 (1977).
[33] Th. Fauster, R. Schneider, H. Dürr, G. Engelmann and E. Taglauer, "Thermally induced disorder on a Cu(110) surface studied by low-energy ion scattering and inverse photoemission", *Surf. Sci.*, **189/190**, 610 (1987).
[34] S. G. J. Mochrie, "Thermal roughening of the copper(110) surface: An X-ray diffraction experiment", *Phys. Rev. Lett.*, **59**, 304 (1987).
[35] A. Mroz and S. Mroz, "Temperature effects in directional elastic peak electron spectroscopy for the Cu(011) face: observation of the surface roughening transition", *Surf. Sci.*, **320**, 307 (1994).

[36] P. Statiris, H. C. Lu and T. Gustafsson, "Temperature dependent sign reversal of the surface contraction of Ag(111)", *Phys. Rev. Lett.*, **72**, 3574 (1994).
[37] L. J. Lews, "Thermal relaxation of Ag(111)", *Phys. Rev.*, **B50**, 17693 (1994).
[38] P. D. Ditlevsen, P. Stoltze and J. K. Norskov, "Anharmonicity and disorder on the Cu(110) surface", *Phys. Rev.*, **B44**, 13002 (1991).
[39] Keh-Dong Shiang, "Molecular dynamics simulation of adatom diffusion on metal surfaces", *J. Chem. Phys.*, **99**, 9994 (1993).
[40] J.-K. Zuo, Y.-L. He, G.-C. Wang and T. E. Felter, "High-resolution low-energy electron diffraction study of Pt(110)(1 × 2) to (1 × 1) phase transition", *J. Vacuum Sci. Technol.*, **A8**, 2474 (1990).
[41] T. Sueyoshi, T. Sasaki and Y. Iwasawa, "Reactive oxygen species on Cu(110) – Catalytic CO–O_2 and CO–NO reactions by reactive oxygen species at low temperatures", SHOKUBAI **37**, 112 (1995) (in Japanese).